INTERNATIONAL JOURNAL FOR NUMERICAL AND ANALYTICAL METHODS IN GEOMECHANICS
Int. J. Numer. Anal. Meth. Geomech., **23**, 1121–1140 (1999)

PILE DRIVING BY NUMERICAL CAVITY EXPANSION

MOUNIR E. MABSOUT, SALAH M. SADEK AND TOUFIC E. SMAYRA

Department of Civil and Environmental Engineering, American University of Beirut, Beirut, Lebanon

SUMMARY

A cavity expansion procedure for the simulation of pile driving is presented and assessed in this paper. The analysis uses a non-linear finite-element model and the penetration of the pile into the soil is simulated by a radial opening of the soil around the pile. The case of a pile advanced by expansion will be compared to a similar pile subjected to computational driving (referred to, respectively, as 'expanded' and 'driven' piles for convenience). The state of stress and deformation, and the evolution of pore-water pressure in the soil will be monitored for the expanded and driven piles. Further computational driving will be applied to both cases and the pile response and soil resistance will be compared. The computational cost of advancing the pile by expansion will finally be investigated. Copyright © John Wiley & Sons, Ltd.

KEY WORDS: pile driving; finite element analysis; cavity expansion; bounding-surface plasticity; soil–structure interaction

INTRODUCTION

A study of pile driving by the finite-element method has been recently presented.[1,2] The model developed by Mabsout and Tassoulas[1] described a rational approach which addresses the driving of a closed-end round pile in clay. The model was extensively applied by Mabsout *et al.*[2] in the case of a prebored concrete pile driven in normally consolidated clays and it was demonstrated that the results obtained were consistent and plausible with approximate methods currently used. However, the computational cost of the analyses was found excessive and it was noted that the current capabilities may limit the applicability of the model in day-to-day practice.

An alternative simple approach for the analysis of pile driving by finite-element cavity expansion is suggested in this paper. Whereas the idea of numerically expanded cavity to model pile penetration is not new,[3,4] it was mainly directed towards predicting (matching) experimental results.[5] While some numerical results were different from those of the experiment, they displayed a consistent pattern. These differences were attributed to several factors, mainly to inadequate modelling of the test boundary conditions. In the present work, the cavity expansion procedure will be compared to the driving model developed by Mabsout and Tassoulas,[1] serving therefore to assess this simpler approach and validate it as an alternate and practical tool for numerical pile penetration.

The state of stress and strain induced in the soil by a driven pile has commonly been estimated by approximate analytical techniques such as the cavity expansion approach. The stress and

* Correspondence to: Mounir E. Mabsout, Department of Civil and Environmental Engineering, Faculty of Enineering and Architecutre, American University of Beirut (AUB), 850 Third Avenue, 18th Floor, New York, New York 10022, U.S.A. E-mail: mounir@aub.edu.lb

CCC 0363–9061/99/111121–20$17.50

Received 30 April 1996
Revised 20 November 1998

strain paths resulting from a cylindrical cavity in the form of the penetrated pile are therefore predicted and further analysis on pile capacity can be performed. In comparison, the present analysis simulates the case of a driven pile by a non-linear cavity expansion using the finite-element method. The cavity is gradually expanded by radially displacing the soil to reach an opening in the shape of the pile. The rationale behind the suggested approach is that, beyond the driving of the pile and as the dynamic effects subside, the changes in the soil are dominated by its radial deformation.

The numerical cavity expansion approach will be assessed by investigating the state of the soil in both cases of expanded and driven piles. Whereas the soil behaviour will be similar for the two cases, additional driving applied to expanded and driven piles will lead to similar responses. The soil resistance exhibited in the course of driving will also be investigated.

The analyses presented in this paper will be limited to closed-end, round, concrete piles with conical tips, driven in undrained normally consolidated clay.

THE PILE-DRIVING MODEL

Soil model

Among the many different models used to predict soil behaviour, the bounding-surface-plasticity model[6,7] for isotropic, cohesive soils, was selected in the analyses presented herein. The model, which is based on the principles of critical-state soil mechanics, has been successfully applied to predict the behaviour of clays under complex loading. The model relates effective stress to strain in invariant space. The total stress σ_{ij}^{t} in saturated clays is obtained by adding the pore-water pressure u to the effective stress σ_{ij} so that, in rate form,

$$\dot{\sigma}_{ij}^{t} = \dot{\sigma}_{ij} + \dot{u}\delta_{ij} \tag{1}$$

where δ_{ij} is the Kronecker delta (compressive stresses are positive).

Completely saturated clay, where no flow of pore fluid occurs in the short term, implies ideal undrained conditions. Such clay, therefore, exhibits only a small change of volume due to the slight compressibility of the soil-water mixture.[8] Denoting by Γ the bulk modulus of mixture, the pore-water-pressure rate $\dot{u}$ can be expressed in terms of the small volume change ε_{mm} as

$$\dot{u} = \Gamma\varepsilon_{mm} \tag{2}$$

The implementation of the bounding-surface model requires the determination of 13 parameters which can be obtained from specific calibration tests.[7] The first six parameters are typical critical-state soil mechanics variables obtained directly from tests (consolidation and rebound slopes λ and κ, slopes of critical-state lines in triaxial extension and compression M_e and M_c, and shear modulus G or Poisson's ratio v); two shape parameters, R and C, determine the geometry of the elliptical bounding surface. The parameter R describes the centre of the ellipse and the parameter C describes the centre of projection of the actual stress state into the image stress state on the bounding surface; the last five parameters (h_c, h_e, s_p, a, w) are required to describe the hardening function, determined by the shape of the stress–strain curves for plastic hardening and softening. h_c and h_e are shape hardening parameters related to triaxial compression and extension, respectively. s_p determines the elastic nucleus ($s_p = 1$ for vanishing elastic range condition). a and w are model parameters which control the behaviour of the hardening function at high overconsolidated ratios. Details on the model formulation and implementation are presented in Ref. 9.[9]

Table I. Bounding-surface clay parameters[7]

Parameter	Value
λ	0·15
κ	0·018
ν	0·30
M_e	1·25
M_c	0·95
R	2·42
C	0·70
s_p	1·60
h_c	60·0
h_e	60·0
A	1·20
W	5·00

Towards verification of the bounding-surface model as implemented for the purposes of the present study, simulations of the response of undrained clay in triaxial tests were carried out[9] at various overconsolidation ratios using the parameter values given in Table I. These parameters correspond to a laboratory prepared kaolin reported by Kaliakin and Dafalias.[7]

The numerical simulation results were found to be identical to the plots given by the latter source, which, in turn, are in close agreement with test results.

Finite-element model

The pile-driving model refers to the axisymmetric finite-element mesh described in Figure 1, where the pile is prebored at 18 m. The discretization is based on the conventional eight-node isoparametric element.

The 50 cm round concrete pile is 20 m long and its parabolic tip extends over a depth of 1 m. Since experience has shown that it will have little deformation in the course of driving, the pile is assumed linear elastic with a modulus of elasticity E_c equal to $24{\cdot}8 \times 10^6$ kPa for normal-strength concrete.

It is expected that the soil in the vicinity of the pile will undergo large deformations as a result of the pile penetration. The inelastic behaviour of the soil is treated by the bounding-surface model for cohesive soils. The clay parameters given in Table I will be considered in the analyses and the soil will be assumed in a normally consolidated state. The procedure for the geometrically non-linear analysis employed in this work is based on the approach developed by Nagtegaal[10] and involves an updated Lagrangian formulation.

For the driving problem, the blow of the hammer is simulated by a forcing function applied at the top of the pile. This function, shown in Figure 2, has been selected from a paper by Goble *et al.*[11] in which a concrete pile of about the same area (0·45 m × 0·45 m) and length (22·5 m) is considered. It has been reduced by 20 per cent since its application in selected driving cases lead to excessive tensile stresses in the pile during part of the blow that could lead to its breakage.[2] While the forcing function selected lasts approximately 0·04 s, the effect of the blow, as is demonstrated later, will be longer. Integration of the equations of motion for the time-domain dynamic problem is performed using the constant-average-acceleration approach.

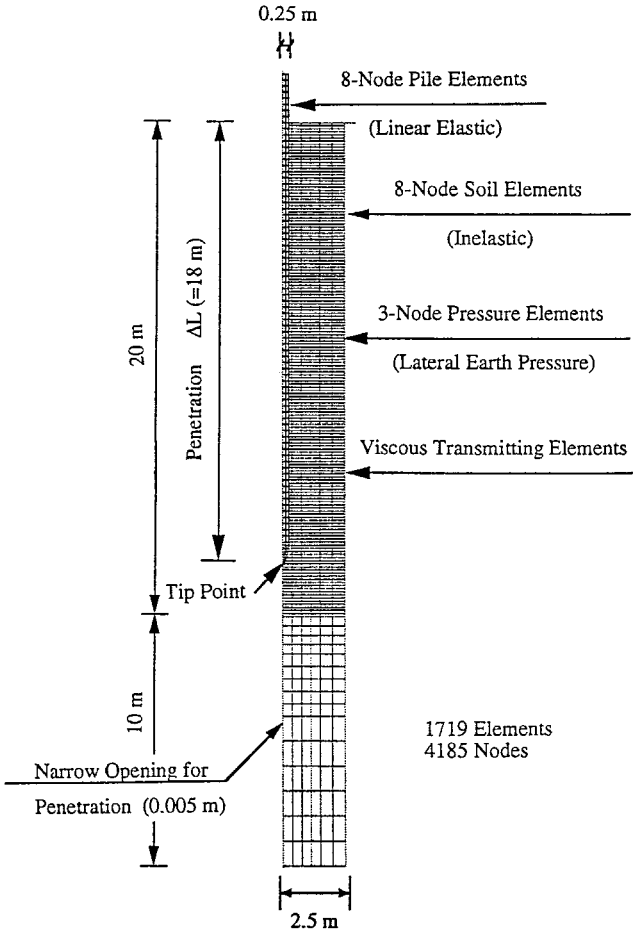

Figure 1. Axisymmetric finite-element discretization of pile–soil system

As shown in Figure 1, a narrow opening of 0·005 m (1 per cent of pile diameter) is provided below the tip of the pile to facilitate the computational penetration of the pile upon driving.

Suitable modelling of the pile–soil interface is required to represent the pile penetration during driving. The slideline formulation described by Hallquist *et al.*[12] and Schwer *et al.*[13] is used in the present study. This contact algorithm, based on the penalty method, permits large relative sliding between the pile and soil, and allows separation if tension occurs along the interface. As penetration is detected, sliding friction of the Coulomb type is modelled.

The modelling of friction between pile and soil is based on the following approach suggested by Mabsout *et al.*[2] Conventionally, the assumption is made that the side resistance τ_s is a percentage of the undrained shear strength c_u of the remolded clay around the shaft:[14]

$$\tau_s = \alpha c_u \tag{3}$$

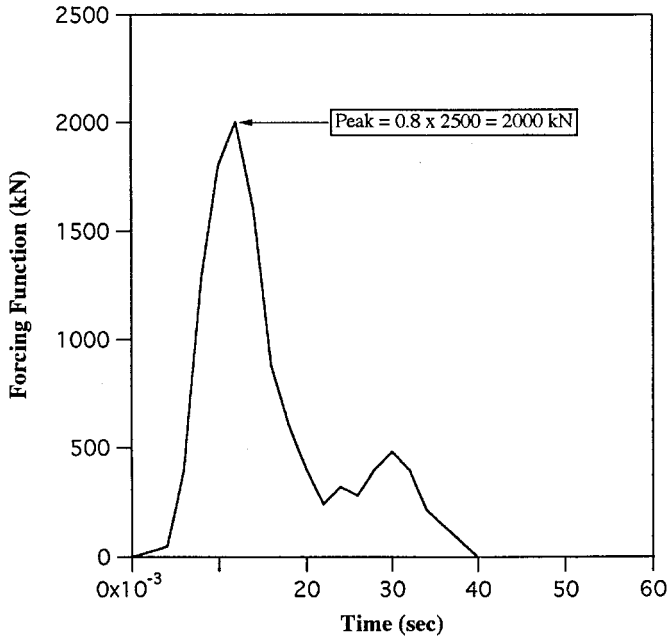

Figure 2. Forcing function simulating hammer blow[10]

where the adhesion factor α depends on the strength of the soil and on the method of installation of the pile. Based on a literature review by Mabsout *et al.*[2], the value of α of 0·65 is selected for use in the driving analyses of prebored piles in normally consolidated undisturbed clays. Computationally, the adhesion τ_s can alternatively be simulated using an equivalent Coulomb-friction expression in terms of total stress. The so-called total friction coefficient μ can therefore be computed from the following equation:

$$\tau_s = \alpha c_u = \mu \sigma_r^t = \gamma Z \tag{4}$$

where the lateral earth pressure coefficient is taken equal to 1, and the total unit weight of the soil γ is constant over the depth Z(m) and equal to 19·41 kN/m^3. The undrained shear strength of the normally consolidated clay of Table I is evaluated from the stress paths of the bounding-surface simulations of triaxial compression tests at various confining pressures. The tests lead to a linear strength $c_u = 2{\cdot}87Z$ (kPa). Therefore, referring to equation (4), a constant value of about 0·1 is obtained for μ. It should be recognized that μ is expected to be much lower in regions where the clay is disturbed during driving, with pore-water pressure build-up. Such will be the state of the soil in the vicinity of the tip. For prebored piles, the coefficient of 0·1 will be suitable in the shaft region where disturbance is minimal. The analysis will therefore be performed to limited amount of driving. For a substantial penetration, such as in the case of fully driven piles, an effective stress approach should be used in the modelling of the side friction. This topic is currently under investigation. It is also worth mentioning that the soil resistance (shaft + tip) exhibited during driving will allow computation of the pile capacity immediately after driving. It is not within the scope of this paper to investigate the pile capacity as consolidation occurs with time. Such

analysis would require the coupling of the current model with the solution of the diffusion equation.

Since the infinite soil mass is modelled by a mesh of finite extent, special absorbing boundaries are introduced at the soil far field (Figure 1); the role of such viscous-type boundaries is to transmit the incident waves resulting from the driving process, and, therefore, prevent their reflection, thus avoiding a spurious response. The formulation of these boundaries depends on the pressure-wave and shear-wave velocities in the soil and is given in Reference 2. The lateral soil pressure applied on the radial boundary is modelled using pressure elements.

The mesh discretization and the finite extent of the domain considered in Figure 1 have been addressed and found suitable for the driving analyses.[2]

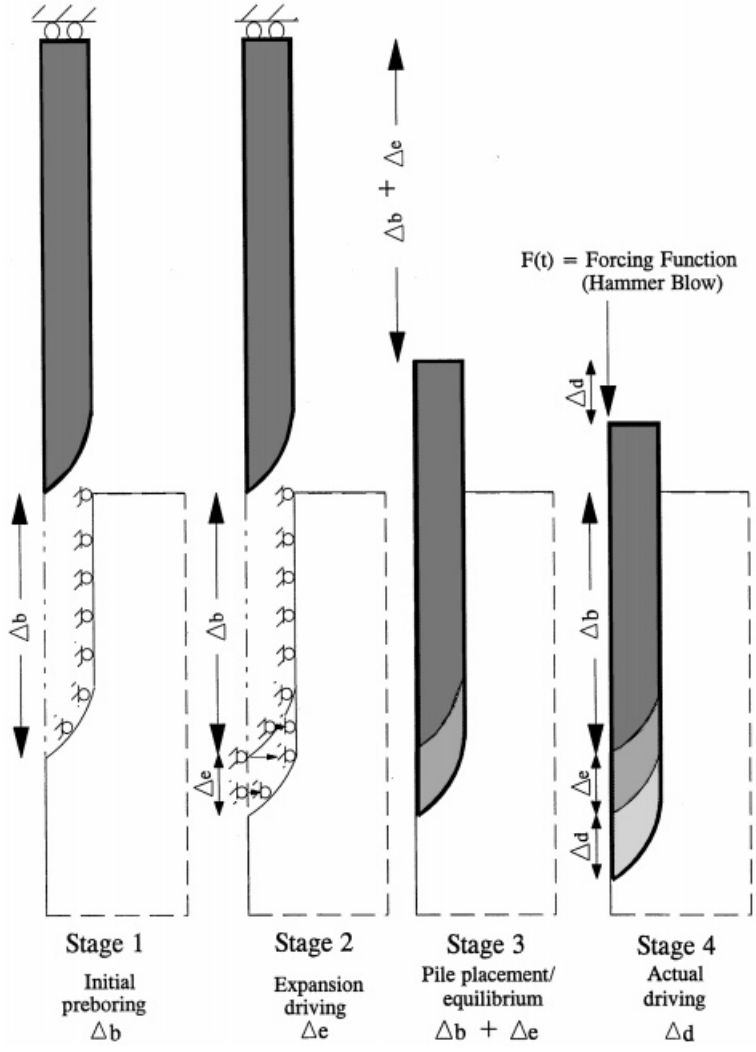

Figure 3. Cavity expansion and actual driving procedures (not to scale)

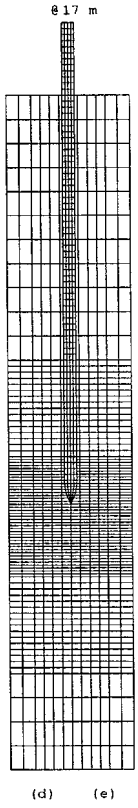

Figure 4. Simplified finite-element mesh used in analyses

NUMERICAL CAVITY EXPANSION PROCEDURE

The basis for the cavity expansion procedure is to simulate the state of stress and deformation of the soil by radially expanding a cavity in the shape of the penetrated pile rather than computationally driving it to that level of penetration. This is explained by the fact that, in the latter case, the change in the state of the soil is due mainly to its radial displacement resulting from the pile penetration; the dynamic effect of the driving is therefore considered to have little effect on the state of a soil once a blow subsides. It should be noted that the expansion procedure should apply in typical low-friction cases where no soil dragdown occurs while driving the pile. The cavity expansion procedure is applied using a static version of the finite-element model described earlier.

The intent is to apply a cavity expansion to the case of an unpenetrated pile. Since the current study aims at comparing the expansion to the actual driving of a pile, the case of driving a pile that is already prebored will rather be considered. This is due to the limitations imposed by the current friction modelling which, as described earlier, would not apply for substantial driving.

As stated earlier, the profiles of the initial total stress $\sigma^t(Z)$ and undrained shear strength $c_u(Z)$ of the normally consolidated clay used in the study (Table I) are evaluated as 19·41 and 2·87 Z (kPa), respectively, where Z is the depth in meter. The state of stress in the soil is assumed to be

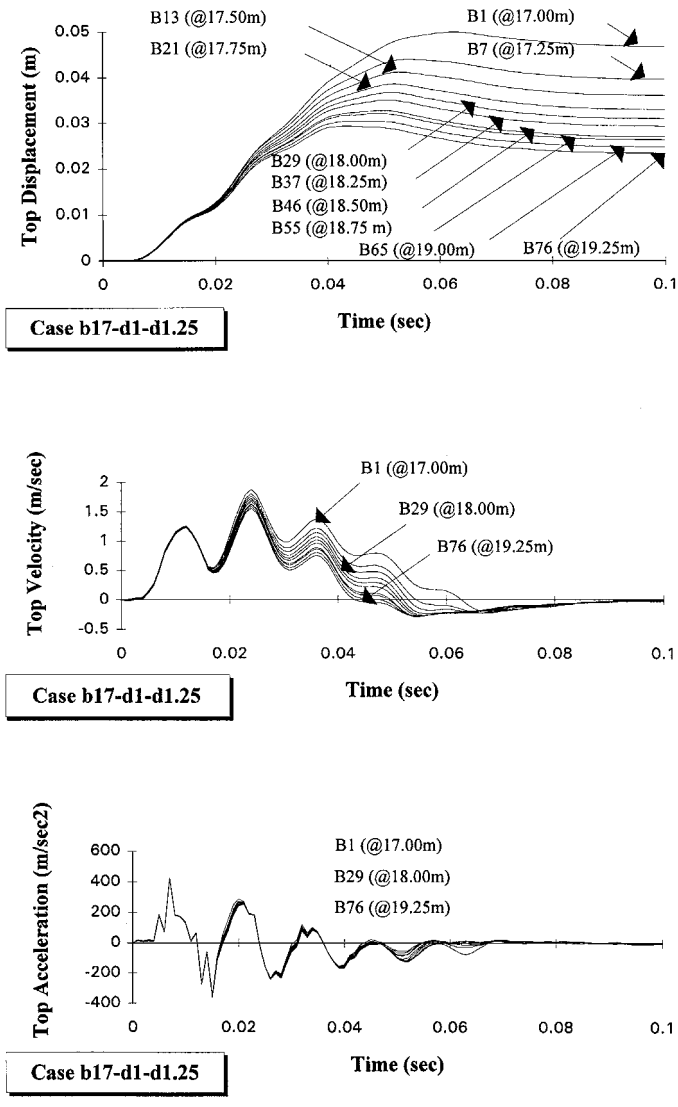

Figure 5. Pile top displacement, velocity and acceleration for case b17-dl-dl.25

the same following the installation of the prebored pile, based on the recognition that little remolding of the soil will take place around the pile shaft.

As shown in Figure 3, the preboring level of the pile is denoted by Δb (Stage 1). A quasi-static expansion of the soil is then performed while the pile is retained from penetration (Stage 2); this is computationally implemented by applying an incremental displacement-controlled radial loading on the soil over a specified depth Δe. This second stage is terminated when the radius of the cavity becomes equal to the one of the pile; Δe will thereafter define the initial driving level

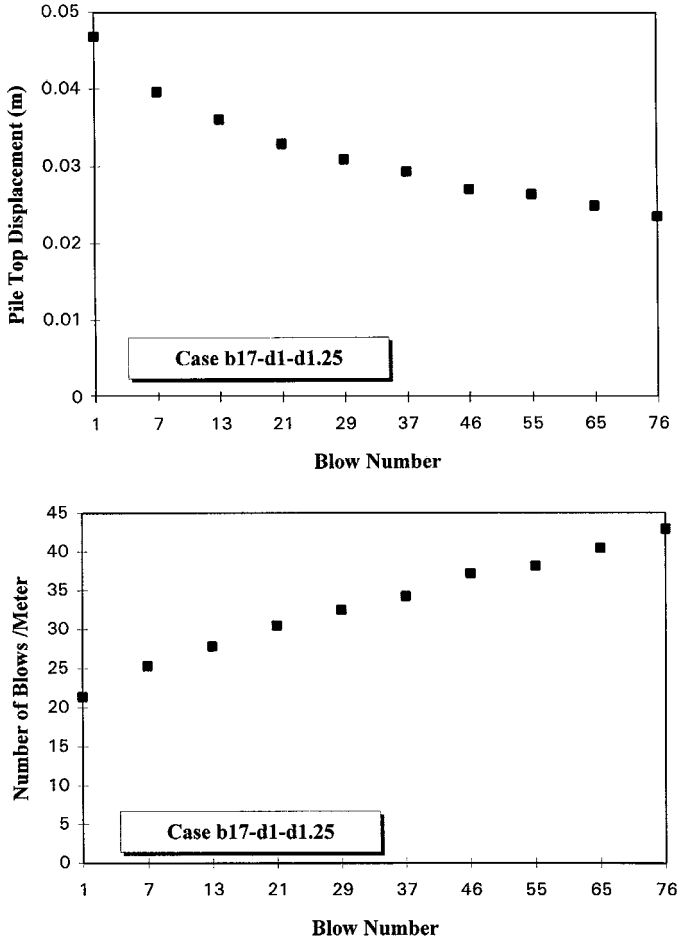

Figure 6. Pile top set or blows/meter versus blow number for case b17-dl-dl.25

performed by expansion. Stage 3 consists of displacing the pile down to the level of the cavity and releasing it so as to leave the system reach equilibrium under its self-weight. This will lead to a minimal disturbance in the soil and small additional penetration δ (or uplift-δ) is obtained; δ is not shown in Figure 3. In Stage 4, computational driving can be performed starting from $\Delta b + \Delta e$, and an additional driving penetration Δd is obtained. This procedure is summarized by: Preboring Δb, expansion driving Δe, and actual driving Δd. It will be referred to thereafter as $b(\Delta b) - e(\Delta e) - d(\Delta d)$.

The b–e–d case described in Figure 3 should be compared to a b–d–d case. While preboring Δb in Stage 1 is the same for both cases, Stage 2 in b–d–d consists of driving $\Delta d1$ that is equivalent to Δe simulated by expansion in b–e–d ($\Delta d1 = \Delta e$). Additional driving $\Delta d2$ is applied in Stage 3 of b–d–d ($\Delta d2$ is equivalent to the Δd of the b–e–d case).

The advantage of the proposed procedure (b–e–d) is in the stage of driving by expansion Δe which will require significantly less computational time than in the driving stage $\Delta d1$ in b–d–d.

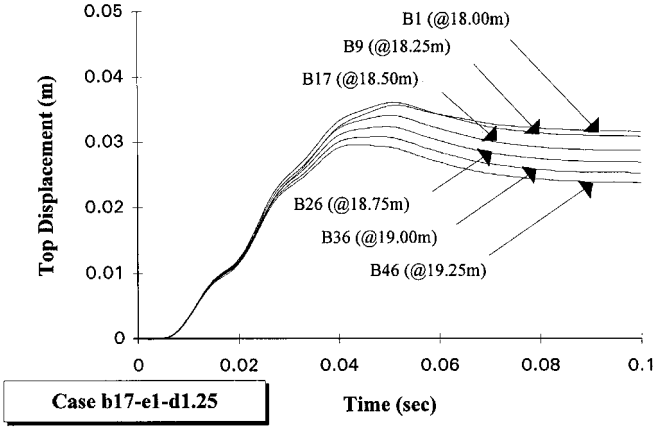

Figure 7. Pile top displacement for case b17-el-dl-25

This would especially be the case when substantial driving is required. The computational advantage will be assessed in a later section.

CASES ANALYSED

Referring to the description outlined in the previous section, the following cases are considered in the analyses:

(1) b17-e1-d1.25: Referring to Figure 3, this case designates a pile that is prebored to the level of 17 m, driven by expansion 1 m (to 18 m), and actually driven an additional 1·25 m (reaching 19·25 m).
(2) b17-d1-d1.25: In this case, the pile is similarly prebored to 17 m, driven 1 m (to 18 m) for comparison with the e1 of the previous case, and similarly driven 1·25 m (reaching 19·25 m).

Since both cases above will start from a preboring depth (17 m), it is expected that major distortions in the soil will be limited to a zone near the driven tip. A fine mesh is therefore needed in the vicinity of the pile tip, while a coarser mesh could be used in the zones of least soil disturbance (away from the pile tip). The axisymmetric mesh shown in Figure 4 was adopted to reduce the computational time. The discretization is shown on both left and right sides of the axis for convenience; left and right sides will later refer to the driven (d) and expanded (e) cases, respectively, for comparative display of results. Results from the driving using this mesh (2285 nodes) and the one shown in Figure 1 (4185 nodes) were nearly identical.[15] It should be noted that the discretization in Figure 4 was not modified in the radial direction. A coarser discretization in the latter direction lead to inaccurate results when assessed with the original mesh.

In the time-domain dynamic analyses, the time step of 0·001 s was found suitable.[1] In the static expansion analysis, a radial displacement step of 0·25 cm is originally adopted to reach a cavity equal to the radius of the pile (25 cm) in 100 steps. However, as the severity of the problem increased during opening (high non-linear behaviour of soil), an adaptive algorithm was introduced to gradually reduce the step (by half) as needed. When convergence allows, an increase in the displacement step is then tolerated to a maximum of 0·25 cm.

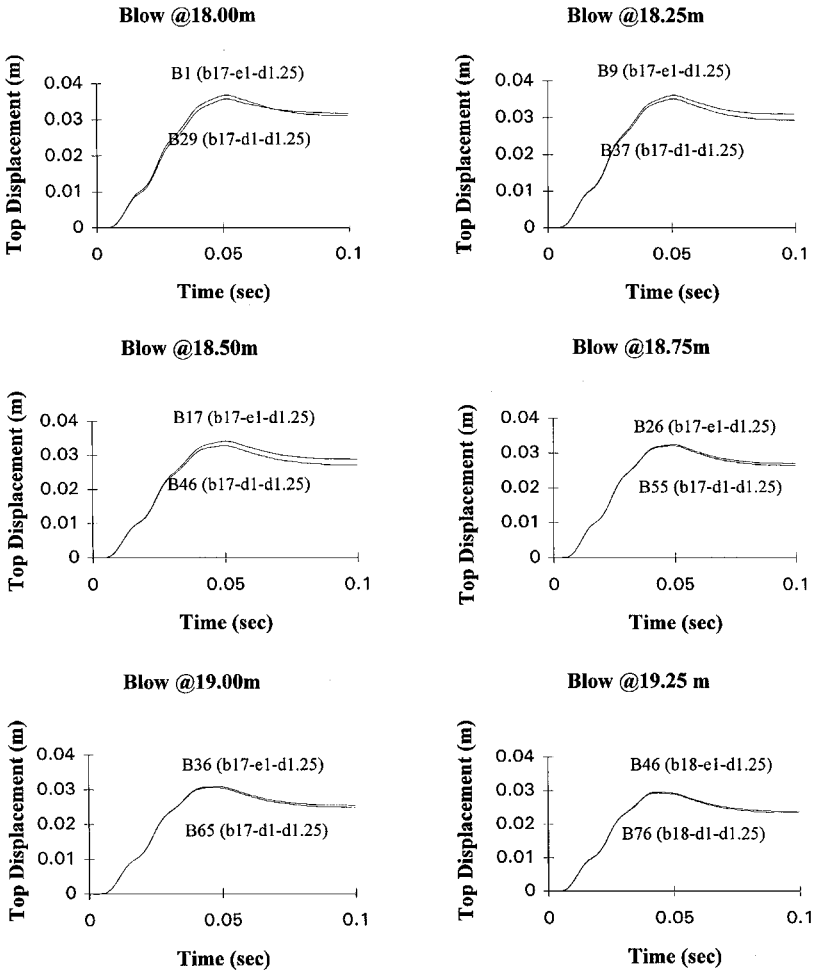

Figure 8. Comparison of pile top displacement for cases b17-dl-dl.25. and b17-el-dl-25

ANALYSIS AND RESULTS

Pile-driving response

The results of the driving response of the two cases considered are first presented and assessed independently. A comparison of the two cases is performed later.

A series of 76 blows was applied at the top of the pile for case b17-d1-d1.25, starting at a preboring depth of 17 m and driving the pile until 19·25 m, for a total penetration of 2·25 m. The plots of pile top displacement, velocity, and acceleration are shown versus time in Figure 5, for blows at 0·25 m penetration intervals (from blow B1 at 17·00 m to blow B76 at 19·25 m). It is worth noting the decrease in the pile permanent set with each blow. This is

Table II. Pile set at end of blow

Case	b17-d1-d1.25		b17-e1-d1.25	
Penetration (m)	Blow	Pile set (m)	Blow	Pile set (m)
18·00	B29	0·0308	B1	0·0315
18·25	B37	0·0292	B9	0·0308
18·50	B46	0·0269	B17	0·0286
18·75	B55	0·0262	B26	0·0268
19·00	B65	0·0247	B36	0·0252
19·25	B76	0·0233	B46	0·0237

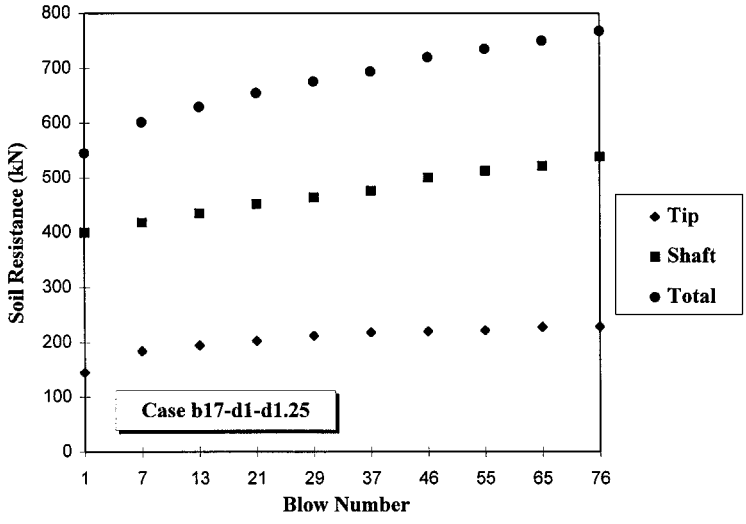

Figure 9. Total, shaft, and tip soil resistances for case b17-dl-dl.25

further clarified in the plot of the decreasing pile set with the blow number, or, inversely, by the increasing number of blows required to penetrate the pile a unit meter (given by 1/set) versus the blow number, as shown in Figure 6. Namely, this pile set decreased from 0·0468 m (requiring 21·3 blows/m) for blow B1 (at 17·00 m) to 0·0233 m (requiring 42·9 blows/m) for blow B76 (at 19·25 m). This expected trend indicates, as will be shown later, that the soil resistance (or pile capacity) increases with driving. It is also worth noting that the computation in a blow is stopped at 0·1 s when the velocity is about zero, far beyond the duration of the forcing function (0·04 s).

A similar set of plots for pile response can be obtained for case b17-e1-d1.25.[15] The pile displacement response is shown in Figure 7. In this case, where the driving through the first meter is simulated by cavity expansion (e1), the first blow B1 is at 18 m and the last blow B46 is at

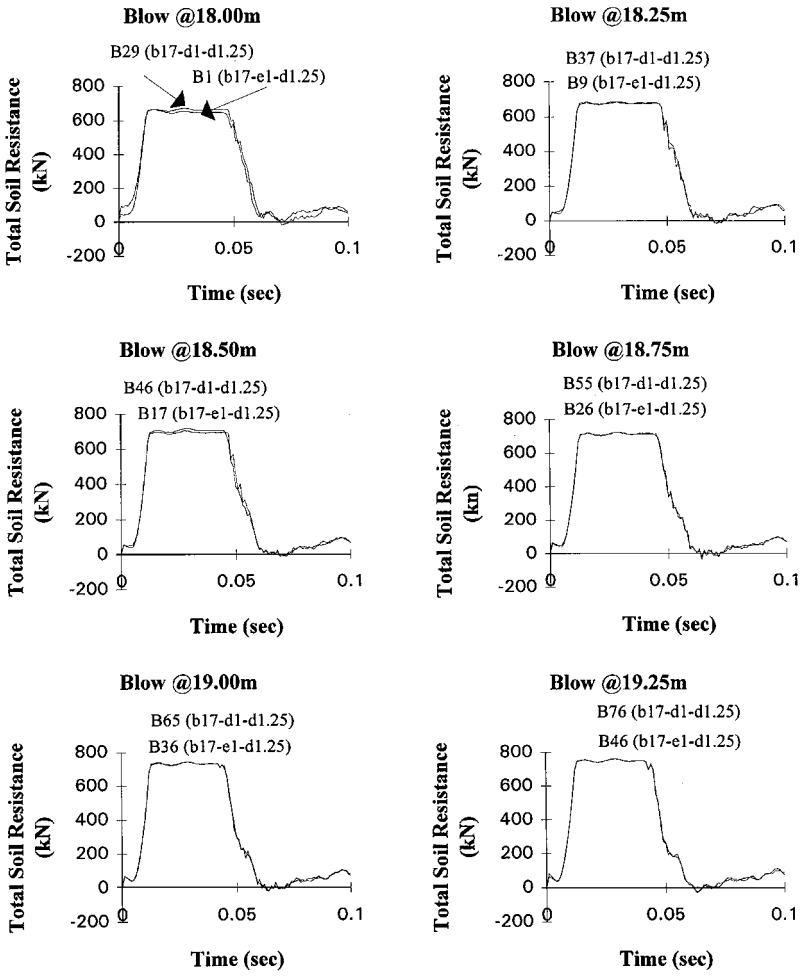

Figure 10. Comparison of total soil resistance for cases b17-dl-dl.25 and b17-el-dl.25

19·25 m. It is noted, therefore, that blows B1 and B46 in this case are level-wise equivalent, respectively, to blows B29 and B76 of case b1-d1-d1.25.

The results for pile top displacement are compared in Figure 8, starting at 18 m and until 19·25 m. The results of the pile set at the end of the corresponding blows are also listed in Table II. It is clearly observed that the plots of pile top displacement (and pile set) at equal levels of penetration are about the same for cases b17-d1-d1.25 (driven) and b17-e1-d1.25 (expanded). In particular, at a level of 18 m, the correlation of displacement responses is very reasonable between blow B29 of b17-d1-d1.25 and blow B1 of b17-e1-d1.25, just beyond the initial 1 m driving/expansion. In comparison, the set of a pile prebored to 18 m (b18) was computed as 0·039 m (Reference 2), indicating a weaker response than for the driven or expanded cases ($\sim$ 0·031 m). Similar patterns have been obtained for velocity and acceleration responses.[15]

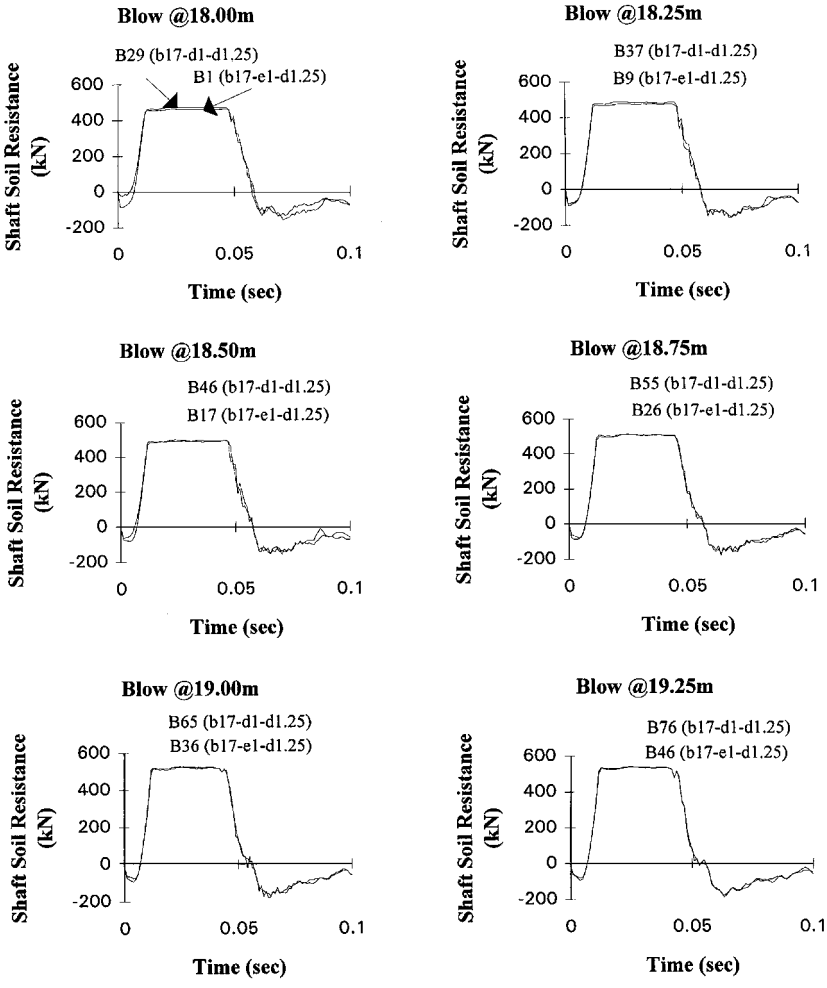

Figure 11. Comparison of shaft soil resistance for cases b17-dl-dl.25 and b17-el-dl.25

Soil resistance

The decrease in the pile top set with the number of blows shown in the previous section indicates that an increase in the static soil resistance (or pile capacity) has occurred with the penetration of the pile as it is driven. In particular, this is demonstrated in Figure 9 for case b17-d1-d1.25 in the plot of the total, shaft, and tip soil resistances versus blow number, at intervals of 0·25 m penetration.

The comparison of soil resistances for the two cases considered is shown in Figures 10–12. These plots are consistent with the ones obtained for pile displacement as they indicate close results for cases b17-d1-d1.25 and b17-e1-d1.25. The total soil resistance was computed as

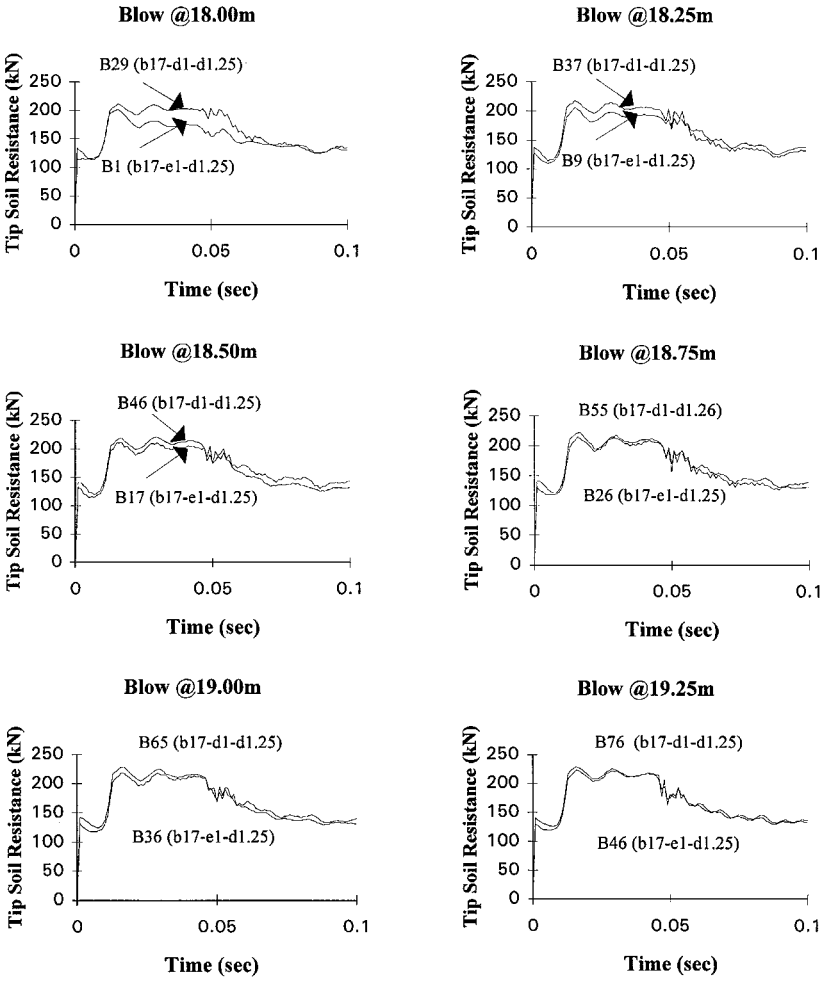

Figure 12. Comparison of tip soil resistance for cases b17-dl-dl.25 and b17-el-dl.25

660 kN at 18 m (455 kN shaft + 205 kN tip) in comparison to 590 kN for a prebored pile at 18 m (b18).

State of deformation and stress in soil

The state of stress and deformation is traced and compared for cases b17-d1-d1.25 and b17-e1-d1.25 at penetration levels 17, 18, and 19 m. These cases are referred to, respectively, as (d) and (e) in Figures 13–15.

The deformed meshes are shown in Figure 13 in a close-up view near the pile tip. As can be observed after 1 m driving/expansion (at 18 m), the deformed meshes are highly distorted for both the (d) and (e) cases. It should be noted, however, that the distortion in case (d) tends to drag the

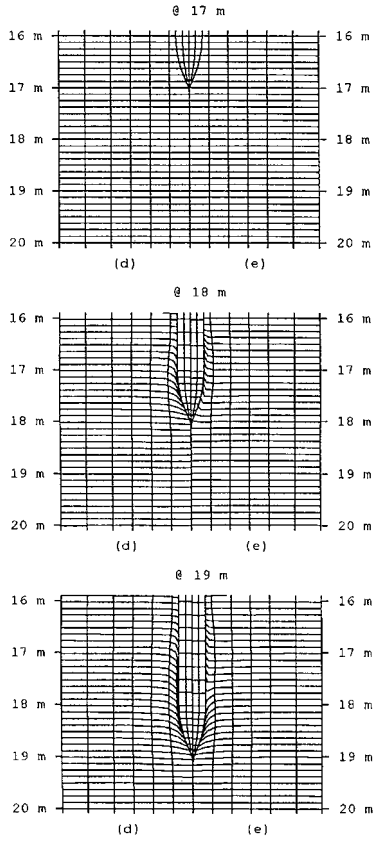

Figure 13. Deformed meshes for cases b17-dl-dl.25 (left, d) and b17-el-dl.25 (right, e); close-up view around the tip

soil slightly down as the tip penetrates, while case (e) shows an expansion upward and downward of the elements around the pile tip. This was noticed also in the sign of the shearing strains and stresses (rz). The dragdown in case (d) is accentuated by the current modelling of the side friction, which, as explained earlier, does not account for the reduction in the pile–soil friction coefficient in regions of disturbed soil. All other normal strains and effective stresses (r, θ, and z) were close for the (d) and (e) cases. The prediction of the change in mean effective stress p and pore-water pressure u build-up are of major importance to geotechnical engineers as they relate to the strength of the soil; these changes can be predicted by the driving/expansion models and are shown in close-up views in Figures 14 and 15. Good agreement was found between the driven and expanded cases. The mean effective stress decreased, especially around the tip, by up to 100 kPa; conversely, the pore-water pressure increased by about 300 kPa around the tip, which is nearly twice the initial mean effective stress at the tip.

Finally, once driving is performed from 18 to 19 m, the behaviour of the soil in cases (d) and (e) tends to be very similar.

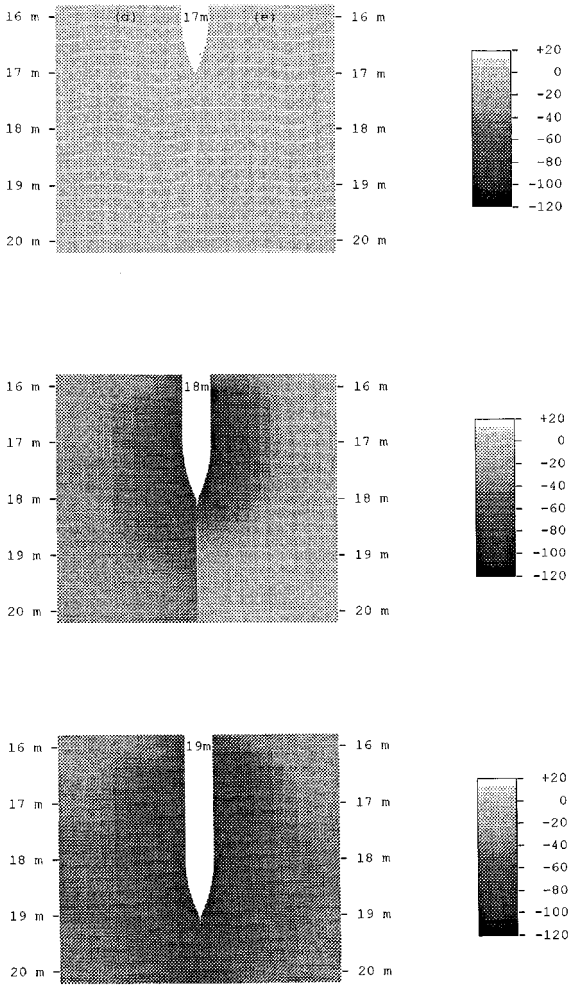

Figure 14. Change in mean effective stress p for cases b17-dl-dl.25 (left, d) and b17-el-dl.25 (right, e); close-up view around the tip

COMPUTATIONAL TIME

The computation for one driving blow was stopped when it subsides at 0·1 s. With a time step of 0·001 s, 100 steps are required per blow. The computer time (Pentium 90 Mhz) for the blow was about 2·5 h (2·3–2·7 h); one time step is therefore equivalent to 0·025 h (about 1·5 min). Moreover, it was found that the displacement step in the expansion case takes similarly about 0·025 h.

The time steps and equivalent computer time are compared in Table III. This comparison is made essentially to show the advantage of the expansion procedure (b17-e1-d1.25) as an alternative to the actual driving (b17-d1-d1.25). The time required by the 1 m expansion is 17·4 h

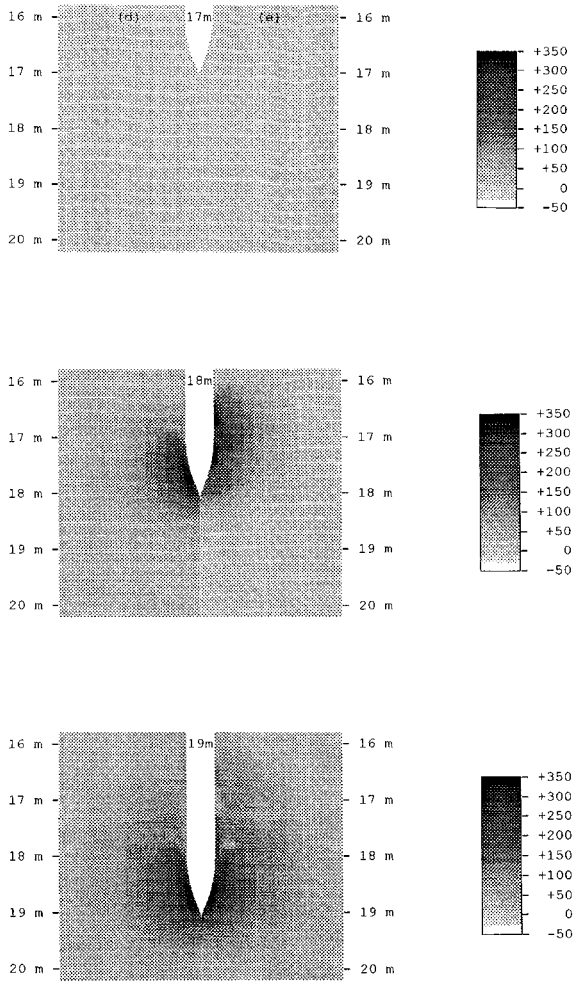

Figure 15. Change in pore–water pressure u for cases b17-dl-dl.25 (left, d) and b17-el-dl.25 (right, e); close-up view around the tip

(696 steps) which is about four times less than the one required by driving 1 m (70 h, 2800 steps for 28 blows). The time required for driving both cases an additional 1·25 m is about the same since these have become equivalent cases (112.5–117.5 h, or 45–47 blows).

One should note here that the saving in computer time (about 4 times) indicated above was for a penetration of 1 m only. In the event that a pile is analysed for a larger amount of penetration (say driving the full 18 m, with no preboring), about the same time would be required for the expansion procedure (same radial opening), while the time for driving the 18 m would be tremendous (hundred of blows or tens of thousand steps required); this would then clearly explain the reason for adopting the alternative of driving by expansion.

Table III. Comparison of time steps and equivalent computer time

	b17-d1-d1.25			b17-e1-d1.25		
Level	Process	Time steps	Computer time (h)	Process	Time steps	Computer time (h)
17·00–18·00 m	Driving (1 m, 28 blows)	2800	70	Expansion (1 m)	696	17·4
18·00–19·25 m	Driving (1·25 m, 45 blows)	4500	112·5	Driving (1·25 m, 47 blows)	4700	117·5

SUMMARY AND CONCLUSIONS

A simple model for the simulation of pile driving by finite-element cavity expansion was developed. The non-linear behaviour of the clay was treated by the bounding-surface model. An updated Lagrangian formulation accounted for the large deformations in the soil.

The cavity expansion model was applied to the driving of a prebored pile in undrained normally consolidated clay. The numerical procedure consisted of a radial static displacement of the soil below the pile to provide an opening equivalent to its penetration. The pile was then fitted in the expanded cavity to reach equilibrium. Further dynamic computational driving was applied and the soil resistance, distributed between the side friction along the shaft and bearing below the tip, was computed, serving as an estimate for the static capacity of the pile.

The case analysed by cavity expansion was assessed with a similar pile equally penetrated by dynamic driving. The latter case has been addressed and validated in a previous work. Results of pile response, and soil resistance and behaviour (effective stresses, pore-water pressure, and deformation), were in good agreement, thus validating the expansion procedure as an alternative model for pile driving.

Where the cost of the driving model has been found excessive to the point of limiting its applicability in day-to-day practice, the cavity expansion approach was perceived as a feasible approach. The advantage in computational cost was noted, especially in the case of substantial penetration.

Unlike the dynamic driving model, the proposed simple approach does not address the suitability of the pile-driving system. The appropriateness of the energy delivered by the driving hammer and the pile integrity are not assessed during the expansion phase. This drawback is more relevant in cases where large penetration is simulated. This can be overcome by applying the driving by expansion in stages; the energy delivered by the hammer and the (tensile) stresses in the pile, as well as the pile capacity and soil behaviour, could then be estimated by applying a driving blow following each expansion stage.

It should be finally noted that the model described in this paper applies for continuously driven piles, where driving is rapid and uninterrupted. All results, therefore, pertain to the state of the soil immediately after driving. In particular, the pile capacity is estimated prior to the consolidation and regain of strength in the soil. A coupling of the model with the diffusion equation would then present a rational solution for the capacity of single piles in saturated clays as a function of time.

ACKNOWLEDGEMENTS

The research reported in this paper was supported by the University Research Board of the American University of Beirut (AUB). Computational resources were provided by the Faculty of Engineering and Architecture at AUB.

REFERENCES

1. M. E. Mabsout and J. L. Tassoulas, 'A finite element model for the simulation of pile driving', *Int. J. Numer. Meth. Geomech. Engng*., **37,** 257–278 (1994).
2. M. E. Mabsout, L. C. Reese and J. L. Tassoulas, 'Study of pile driving by finite-element method', *J. Geotech. Engng. ASCE*, **121,** 535–543 (1995).
3. M. F. Randolph, J. P. Carter and C. P. Wroth, 'Driven piles in clay — the effects of installation and subsequent consolidation', *Geotechnique*, **29,** 361–393 (1979).
4. M. B. Chopra and G. F. Dargush, 'Finite-element analysis of time-dependent large-deformation problems', *Int. J. Numer. Anal. Meth. Geomech*., **16,** 101–130 (1992).
5. R. C. Fathallah, 'Theoretical and experimental investigation of the behavior of axially loaded single piles driven in saturated clays', *Ph.D. Thesis*, University College, Cardiff, 1978.
6. Y. F. Dafalias and L. R. Herrmann, 'Bounding surface plasticity. II: application to isotropic cohesive soils', *J. Engng. Mech. ASCE*, **112,** 1263–1291 (1986).
7. V. N. Kaliakin and Y. F. Dafalias, 'Simplifications to the bounding surface model for cohesive soils', *Int. J. Numer. Anal. Meth. Geomech*., **13,** 91–100 (1989).
8. L. R. Herrmann, V. N. Kaliakin, C. K Chen, K. D. Mish and Z. Y. Zhu, 'Numerical implementation of plasticity model for cohesive soils', *J. Engng. Mech. ASCE*, **113,** 500–519 (1986).
9. M. E. Mabsout and J. L. Tassoulas, 'A finite element model for the analysis of pile driving', *Research Report*, Offshore Technology Research Center, University of Texas at Austin, 1992.
10. J. C. Nagtegaal, 'On the implementation of inelastic constitutive equations with special reference to large deformation problems', *Comput. Meth. Appl. Mech. Engng*., **33,** 469–484 (1982).
11. G. G. Goble, F. Raushe and G. E. Likins, 'The analysis of pile driving—a state-of-the-art', *Int. Seminar on the Appl. of Stress-Wave Theory on Piles*, A. A. Balkema, Rotterdam, The Netherlands, 1980.
12. J. O. Hallquist, G. L. Goudreau and D. J. Benson, 'Sliding interfaces with contact-impact in large scale, Lagrangian computations', *Comput. Meth. Appl. Mech. Engng*., **51,** 107–137 (1985).
13. R. M. Schwer, R. Rosinsky and J. Day, 'An axisymmetric Lagrangian technique for predicting earth penetration including penetrator response', *Int. J. Numer. Anal. Meth. Geomech*., **12,** 235–262 (1988).
14. M. J. Tomlinson, 'The adhesion of piles driven in clay soils', *Proc. 4th Int. Conf. on Soil Mech. and Found. Engng*., International Society for Soil Mechanics and Foundation Engineering, London, England, Vol. **2,** 1957, pp. 66–71.
15. T. E. Smayra, 'A simplified finite-element approach for the analysis of driven piles', *ME Thesis*, American University of Beirut, Lebanon, 1994.

